



Reductions in
aircraft particulate
emissions

A. J. Beyersdorf et al.

This discussion paper is/has been under review for the journal Atmospheric Chemistry and Physics (ACP). Please refer to the corresponding final paper in ACP if available.

Reductions in aircraft particulate emissions due to the use of Fischer–Tropsch fuels

A. J. Beyersdorf¹, M. T. Timko^{2,*}, L. D. Ziemba¹, D. Bulzan³, E. Corporan⁴, S. C. Herndon², R. Howard⁵, R. Miake-Lye², K. L. Thornhill^{1,6}, E. Winstead^{1,6}, C. Wey³, Z. Yu², and B. E. Anderson¹

¹NASA Langley Research Center, Hampton, Virginia, USA

²Aerodyne Research, Inc., Billerica, Massachusetts, USA

³NASA Glenn Research Center, Cleveland, Ohio, USA

⁴Air Force Research Laboratory, Wright Patterson AFB, Ohio, USA

⁵Arnold Engineering Development Center, Arnold AFB, Tennessee, USA

⁶Science Systems and Applications, Inc., Hampton, Virginia, USA

* now at: Worcester Polytechnic Institute, Worcester, Massachusetts, USA

Received: 24 April 2013 – Accepted: 21 May 2013 – Published: 10 June 2013

Correspondence to: A. J. Beyersdorf (andreas.j.beyersdorf@nasa.gov)

Published by Copernicus Publications on behalf of the European Geosciences Union.

Title Page

Abstract

Introduction

Conclusions

References

Tables

Figures



Back

Close

Full Screen / Esc

Printer-friendly Version

Interactive Discussion



Abstract

The use of alternative fuels for aviation is likely to increase due to concerns over fuel security, price stability and the sustainability of fuel sources. Concurrent reductions in particulate emissions from these alternative fuels are expected because of changes in fuel composition including reduced sulfur and aromatic content. The NASA Alternative Aviation Fuel Experiment (AAFEX) was conducted in January–February 2009 to investigate the effects of synthetic fuels on gas-phase and particulate emissions. Standard petroleum JP-8 fuel, pure synthetic fuels produced from natural gas and coal feedstocks using the Fischer–Tropsch (FT) process, and 50 % blends of both fuels were tested in the CFM-56 engines on a DC-8 aircraft. To examine plume chemistry and particle evolution with time, samples were drawn from inlet probes positioned 1, 30, and 145 m downstream of the aircraft engines. No significant alteration to engine performance was measured when burning the alternative fuels. However, leaks in the aircraft fuel system were detected when operated with the pure FT fuels as a result of the absence of aromatic compounds in the fuel.

Dramatic reductions in soot emissions were measured for both the pure FT fuels (reductions of 84 % averaged over all powers) and blended fuels (64 %) relative to the JP-8 baseline with the largest reductions at idle conditions. The alternative fuels also produced smaller soot (e.g. at 85 % power, volume mean diameters were reduced from 78 nm for JP-8 to 51 nm for the FT fuel), which may reduce their ability to act as cloud condensation nuclei (CCN). The reductions in particulate emissions are expected for all alternative fuels with similar reductions in fuel sulfur and aromatic content regardless of the feedstock.

As the plume cools downwind of the engine, nucleation-mode aerosols form. For the pure FT fuels, reductions (94 % averaged over all powers) in downwind particle number emissions were similar to those measured at the exhaust plane (84 %). However, the blended fuels had less of a reduction (reductions of 30–44 %) than initially measured (64 %). The likely explanation is that the reduced soot emissions in the blended fuel

Reductions in aircraft particulate emissions

A. J. Beyersdorf et al.

Title Page

Abstract

Introduction

Conclusions

References

Tables

Figures



Back

Close

Full Screen / Esc

Printer-friendly Version

Interactive Discussion



Reductions in aircraft particulate emissions

A. J. Beyersdorf et al.

Title Page

Abstract

Introduction

Conclusions

References

Tables

Figures

◀

▶

◀

▶

Back

Close

Full Screen / Esc

Printer-friendly Version

Interactive Discussion



exhaust plume results in promotion of new particle formation microphysics, rather than coating on pre-existing soot particles, which is dominant in the JP-8 exhaust plume. Downwind particle volume emissions were reduced for both the pure (79 and 86 % reductions) and blended FT fuels (36 and 46 %) due to the large reductions in soot emissions. In addition, the alternative fuels had reduced particulate sulfate production (near-zero for FT fuels) due to decreased fuel sulfur content.

To study the formation of volatile aerosols (defined as any aerosol formed as the plume ages) in more detail, tests were performed at varying ambient temperatures (−4 to 20 °C). At idle, particle number and volume emissions were reduced linearly with increasing ambient temperature, with best fit slopes corresponding to $-1.2 \times 10^6 \#(\text{kg fuel})^{-1} \text{ } ^\circ\text{C}^{-1}$ for particle number emissions and $-9.7 \text{ mm}^3 (\text{kg fuel})^{-1} \text{ } ^\circ\text{C}^{-1}$ for particle volume emissions. The temperature dependence of aerosol formation can have large effects on local air quality surrounding airports in cold regions. Aircraft produced aerosols in these regions will be much larger than levels expected based solely on measurements made directly at the engine exit plane. The majority (90 % at idle) of the volatile aerosol mass formed as nucleation-mode aerosols with a smaller fraction as a soot coating. Conversion efficiencies of up to 3.8 % were measured for the partitioning of gas-phase precursors (unburned hydrocarbons and SO₂) to form volatile aerosols. Highest conversion efficiencies were measured at 45 % power.

1 Introduction

Aircraft are a unique anthropogenic source of pollution as they emit at both ground-level and high altitude. Ground-level emissions have an effect on local air quality in regions surrounding airports while emissions at altitude increase cloud cover (through the formation of contrails and aircraft-induced cloudiness) and increase background levels of black carbon which is estimated to be the second strongest contributor to current global warming (Ramanathan and Carmichael, 2008). Excluding newly identified

emissions of lubrication oils (Yu et al., 2012), aircraft particulate emissions (including direct emissions of soot and secondary aerosols formed from the processing and partitioning of gas-phase emissions) are especially linked to the composition of the fuel. Aromatics in the fuel lead to the formation of soot (Bauer and Jeffers, 1988; Richter and Howard, 2000), while fuel sulfur is converted to gas-phase sulfur dioxide (SO₂) and then to particulate sulfate (Tremmel and Schumann, 1999; Lukachko et al., 2008). Thus, changes to the composition of the fuel lead to changes in particulate emissions.

The continued increase in energy usage and political instability in many petroleum-producing countries have increased the demand for alternative aviation fuel research with the belief that the introduction of commercial-scale non-petroleum fuel sources will improve fuel security and stabilize future prices. Current research has focused on the goal of developing “drop-in” fuels allowing for use in aircraft without engine modification (Law, 2012). Possible feedstocks include bio-renewable resources (plants, algae or animal fat) and alternative fossil fuels (such as coal or natural gas). These feedstocks are reformulated to provide a fuel with similar physical properties (such as viscosity and density) as petroleum-derived fuel but likely with distinct chemical compositions.

The production of liquid fuel from coal, natural gas and biomass dates back to the early twentieth century. The first step in this process is the production of syngas (a mixture of CO and H₂) from the feedstock. The syngas can be converted via the Fischer–Tropsch (FT) process to produce hydrocarbons and further processed to produce a fuel with a volatility range similar to JP-8. This process leads to a fuel composed primarily of alkanes with very little aromatic content and no sulfur. These characteristics are beneficial when considering particulate emissions from aircraft engines burning FT fuels as low levels of aromatics have been shown to produce less soot, particularly at low engine power (Corporan et al., 2010; Timko et al., 2010; Lobo et al., 2011), and low sulfur content leads to decreased formation of volatile aerosols (defined as any aerosol formed as the plume ages).

However, it should be noted that while FT fuels result in reduced particulate emissions, the synthesis of FT fuels is likely to produce more CO₂ than the production of

Reductions in aircraft particulate emissions

A. J. Beyersdorf et al.

Title Page

Abstract

Introduction

Conclusions

References

Tables

Figures

◀

▶

◀

▶

Back

Close

Full Screen / Esc

Printer-friendly Version

Interactive Discussion



Reductions in aircraft particulate emissions

A. J. Beyersdorf et al.

Title Page

Abstract

Introduction

Conclusions

References

Tables

Figures



Back

Close

Full Screen / Esc

Printer-friendly Version

Interactive Discussion



standard jet fuel. For example, Jaramillo et al. (2008) estimated lifecycle green-house gas (GHG) emissions for an automotive FT fuel from coal and natural gas that are twice as large as for petroleum-based gasoline. To equalize the GHG emissions it is necessary for FT fuel production facilities to utilize carbon capture and sequestration (CCS) technology and use a low-carbon source of energy (such as nuclear or renewable sources). Alternatively, the use of a biomass feedstock also can reduce GHG emissions relative to petroleum-based fuels (Xie et al., 2011). While it is essential to take into account the feedstock when determining overall emissions, it is believed that reductions in particulate emissions are expected for all alternative fuels with similar fuel composition regardless of the feedstock. Therefore it is important to characterize the particulate emissions produced from burning alternative fuels based on fuel composition and not on the specific production process in order to guide future advancements in production technologies.

To study the effects of FT fuel usage on aircraft gaseous and particulate emissions, NASA sponsored the Alternative Aviation Fuel Experiment (AAFEX). Measurements were made behind a commercial aircraft burning standard JP-8, neat FT and JP-8/FT blended fuels. Particulate emissions are presented here while gas-phase chemistry is presented in Lee et al. (2011) and Santoni et al. (2011). In addition to measurements at the exhaust plane, downwind plumes were sampled to determine the effects of aging on aerosol concentrations and composition including the role of ambient temperature. Emissions from the aircraft's auxiliary power unit (APU) are discussed in Kinsey et al. (2012).

2 Experimental design

The AAFEX experiment was performed at the NASA Dryden Aircraft Operations Facility in Palmdale, California from 20 January–3 February 2009 with participants from Aerodyne Research Inc., the Air Force Research Lab at Wright–Patterson, Arnold Engineering Development Center, Carnegie–Mellon University, the US EPA, Harvard Univer-

sity, Missouri University of Science and Technology, Montana State University, NASA (Dryden, Glenn, and Langley Research Centers), United Technologies Research Center, and the University of California (San Diego). The large collaboration allowed for a variety of measurements and comparison between similar measurements to determine optimal sampling methods. A complete list of instrumentation is provided in the NASA AAFEX Technical Report (Anderson et al., 2011) and measurements used in the present analysis are listed in Table 1. Many of the experimental techniques were based on previous NASA-sponsored experiments including the three tests in the Aircraft Particle Emissions Experiment series (APEX; Wey et al., 2007).

The test aircraft was a DC-8 with four CFM-56-2C1 engines. The aircraft was parked on the tarmac and exhaust inlet probes were placed at 1, 30 and 145 m behind the exhaust planes of the #2 and #3 engines (left and right inboard, respectively; Fig. 1). Samples collected at 1 m were diluted with a concentric flow of dry nitrogen to prevent condensation of water and low-volatility exhaust components. This dilution ratio was typically on the order of 10–20:1. Exhaust drawn into the downstream probes was typically naturally diluted by a factor of 20 or more with background air and was thus analyzed without additional dilution. Stainless steel sample lines carried the exhaust flow from the 1 m and 30 m probes to trailers which housed the research instrumentation. The two 1 m and two 30 m probes were each sampled individually in alternating time periods during the course of a test run. The full instrumentation suite was available to analyze samples extracted at 1 and 30 m whereas the 145 m sample was analyzed with a smaller set of instruments housed in a separate trailer. At 145 m downwind, the exhaust from the left and right engines often merged resulting in a mix between emissions from the two engines. For this reason, data from the 145 m probe are only considered for periods when the same fuel was burned in both engines (i.e., only for JP-8 fuel tests since the alternative fuels were never burned in engine #2).

During testing, the #2 and #3 engines were cycled through a set of eight different power settings from 4% to 100% of maximum rated thrust (fuel flow rates of 0.13–0.96 kg s⁻¹ or 1000–7600 lbh⁻¹), which correspond to the range from ground idle to

Reductions in aircraft particulate emissions

A. J. Beyersdorf et al.

Title Page

Abstract

Introduction

Conclusions

References

Tables

Figures

◀

▶

◀

▶

Back

Close

Full Screen / Esc

Printer-friendly Version

Interactive Discussion



Reductions in aircraft particulate emissions

A. J. Beyersdorf et al.

Title Page

Abstract

Introduction

Conclusions

References

Tables

Figures

◀

▶

◀

▶

Back

Close

Full Screen / Esc

Printer-friendly Version

Interactive Discussion



was leaks in the aircraft fuel system when the neat FT fuels were allowed to sit in the tanks for more than a few hours. This is the result of near-zero levels of aromatic compounds in the neat FT fuels. Aromatics in fuel cause elastomer seals in the fuel system to swell (DeWitt et al., 2008) and thus their absence in the FT fuels resulted in leakage. Leaks were corrected when the neat FT fuel was replaced with JP-8 or the blended fuels.

Complete combustion of fuels would result in CO_2 as the only carbon-containing emission. Based on the carbon content of the fuel, a theoretical CO_2 emission index (EI) can be determined for each fuel varying between $3090 \text{ g CO}_2 \text{ kg}^{-1}$ fuel burned for FT-1 and $3160 \text{ g CO}_2 \text{ kg}^{-1}$ for JP-8. Combustion efficiencies (based on emissions of CO and unburned hydrocarbons – UHCs) above 95 % were seen for all the fuels with efficiencies above 99 % at high power settings (Fig. 2). However, the FT and blended fuels exhibited higher combustion efficiencies than JP-8 at low power settings by approximately 1 % (a response also measured for the combustion of biodiesels; Thaiyasuit et al., 2012). Because of the high combustion efficiencies and the ease of measuring CO_2 , it provides a convenient parameter against which to normalize gas-phase and particulate measurements. For example, the particulate number emission index (EI_N ; particles kg^{-1} or kg^{-1}) can be found by

$$\text{EI}_N = \left(\frac{\Delta N}{\Delta \text{CO}_2 \cdot 10^{-6}} \right) \cdot \left(\frac{M_{\text{air}}}{M_{\text{CO}_2} \rho_{\text{air}}} \right) \cdot \text{EI}_{\text{CO}_2} \quad (1)$$

where ΔN is the enhancement in particle density ($\# \text{ cm}^{-3}$) above background (for particles with diameters larger than 4 nm), ΔCO_2 is the enhancement in CO_2 (ppmv), M_{air} and M_{CO_2} are the molar masses of air and CO_2 , ρ_{air} is the density of air, and the value for EI_{CO_2} is dependent on the fuel used. This equation is similar to that suggested by the Society of Automotive Engineers (SAE) Aircraft Exhaust Emissions Measurement Committee (SAE E31). The same technique can be used to calculate the emission indices of gas-phase SO_2 (EI_{SO_2} ; g kg^{-1}), gas-phase unburned hydrocarbons (EI_{UHC} ,

g kg^{-1}), particulate volume density (EI_V ; $\text{mm}^3 \text{kg}^{-1}$), and particulate masses of black carbon (EI_{BC} ; mg kg^{-1}), sulfate (EI_{SO_4}) and organics (EI_{Org}).

3.2 Engine differences

Because engine particle and gas emissions vary considerably with ambient temperature, particulate measurements behind the test engine were compared to measurements behind the control engine burning JP-8. This approach assumes that the two engines have similar emissions characteristics. To validate this assumption, tests were performed burning JP-8 in each engine. Comparison of the two engines showed similar EI_N values (a test-to-control-engine ratio of 0.86 ± 0.22) but differing EI_{BC} (ratios of 0.56 ± 0.30) with the largest discrepancy at intermediate power settings. Thus, it appears that even though the two engines are of approximately the same age and received the same maintenance and servicing, the control engine simply produced more soot at the mid-power settings. In addition, it is possible that there were differences in particulate losses in the lines running between the two probes and the instrumentation. Because of these differences, test engine data will be used for the further analysis and temperature effects will be discussed separately.

3.3 Direct emissions

As expected based on previous literature reports, UHC emissions were greatest at low power and decreased significantly with increasing power (Fig. 2). Conversely, EI_{SO_2} was fairly constant with power. A small increase in EI_{SO_2} was measured with increasing power; however this could be a result of interference from NO which has a large engine power-dependence. Use of the FT fuels resulted in reductions in EI_{UHC} of 40% and in EI_{SO_2} of over 90%. Blended fuel emissions of UHCs and SO_2 were intermediate between JP-8 and the FT fuels.

Directly behind the engine, aerosol is composed almost entirely of soot due to the high temperatures of the exhaust. The soot is composed of primary spherules which

Reductions in aircraft particulate emissions

A. J. Beyersdorf et al.

Title Page

Abstract

Introduction

Conclusions

References

Tables

Figures

◀

▶

◀

▶

Back

Close

Full Screen / Esc

Printer-friendly Version

Interactive Discussion



Reductions in aircraft particulate emissions

A. J. Beyersdorf et al.

Title Page

Abstract

Introduction

Conclusions

References

Tables

Figures

◀

▶

◀

▶

Back

Close

Full Screen / Esc

Printer-friendly Version

Interactive Discussion



coagulate to form larger soot aggregates. The primary spherules (soot nuclei) form via the HACA (hydrogen abstraction/carbon addition) process which first forms polycyclic aromatic hydrocarbons (PAHs) and then soot (Bauer and Jeffers, 1988; Wang and Frenklach, 1994; McEnally and Pfefferle, 1997). This process is favored at high engine power causing an increase in EI_{BC} (Fig. 3). The EI_V values follow the same trend as EI_{BC} , however the trend in EI_N differs due to varying particle size with power (Fig. 4). Soot mean particle diameter increases from 47 nm at idle to 97 nm at 100 % power. This size shift could be the result of formation of soot from primary spherules; as power increases more spherules are produced increasing the probability of coagulation to form larger soot particles.

As shown in Fig. 3, there is a marked decrease in EI_N , EI_V and EI_{BC} when burning the alternative fuels. The low aromatic content of the alternative fuels results in lower soot formation. JP-8 emissions exceeded those from FT fuels and blends for all parameters measured and at all powers. No trend with respect to power is seen in the EI_{BC} mass reductions with average FT/JP-8 ratios of 0.16 ± 0.06 and Blend/JP-8 ratios of 0.36 ± 0.16 for all powers. However, the largest EI_N and EI_V reductions were seen at mid-powers as a result of a shift in the soot size. These reductions were over 95 % for the neat FT fuels and 85 % for the blended fuels.

The alternative fuels also produced smaller soot particles in comparison to JP-8 (at the same power settings). For example, at 85 % power volume mean diameters (VMDs) of 78, 63 and 51 nm were measured for JP-8, Blend-1 and FT-1, respectively. As discussed earlier, this is the result of reduced number concentration of primary soot spherules in the alternative fuel exhaust causing reduced spherule coagulation. Thus, VMD monotonically increases with EI_{BC} (Fig. 5). The amount of coagulation also causes a shift in the soot effective density (EI_{BC}/EI_V measured by a MAAP and DMA, respectively; DeCarlo et al., 2004). Density calculations are only made for engine powers higher than 65 % due to low soot loadings at low power. For the pure FT fuels, with the lowest soot emissions, the relatively lower level of coagulation results in spherules that are tightly packed (higher density). As the EI_{BC} increase, coagulation increases

and the resulting soot particles have more branching and voids and thus a lower density. This is seen in the central panel of Fig. 5, where density decreases with increasing El_{BC} . However, a dependence on engine power is also seen. Similar densities (near unity) were measured during APEX (Onasch et al., 2009).

The separate dependence on El_{BC} leads to an inverse relationship between VMD and density (Fig. 5, right panel). The trend is also apparent for emissions from a modified PW308 gas turbine engine burning JP-8 and Fischer–Tropsch fuels which emitted larger soot particles (Timko et al., 2010). The dependence of soot density on VMD is in agreement with measurements of synthetic fullerene soot (Gysel et al., 2011) which is often used for calibration of black carbon instrumentation. As seen in the figure, fullerene soot is likely an appropriate surrogate for sub-100 nm aircraft soot particles, but may not be relevant for larger sizes. This is in comparison to Moteki and Kondo (2010), who studied other synthetic black carbon sources and found weaker (or no) correlation between particle size and density.

The differences in particulate emission characteristics observed between the fuels of different aromatic content are expected given the current understanding of soot formation and growth in gas turbine engines. Several studies have shown that the soot production is proportional to fuel aromatic and naphthalene content (Rosfjord, 1987; Chin and Lefebvre, 1990a, b) and inversely proportional to fuel hydrogen content (Sampath et al., 1986; Rosfjord, 1987). Based on the analysis of the AAFEX fuels (Supplement), FT-2 had lower hydrogen (15.1 vs. 15.5 %), higher alkene (3.8 vs. 0 %) and higher aromatic (0.6 vs. 0 %) content than FT-1, all of which suggests that the FT-2 fuel should exhibit greater sooting tendency than the FT-1 fuel (which it does). In addition, the FT-2 had more branched alkanes than FT-1 which promotes sooting (DeWitt et al., 2008). The same trend is true for the blended fuels. In general, good correlation was seen at all power settings between soot production (for El_N , El_V and El_{BC}) and fuel properties with a linear correlation for aromatic content and an inverse relationship versus hydrogen content. Particle emissions were slightly better correlated with fuel aromatic than hydrogen content at all thrust settings. However, because the fuel aromatic and hydro-

Reductions in aircraft particulate emissions

A. J. Beyersdorf et al.

[Title Page](#)[Abstract](#)[Introduction](#)[Conclusions](#)[References](#)[Tables](#)[Figures](#)[Back](#)[Close](#)[Full Screen / Esc](#)[Printer-friendly Version](#)[Interactive Discussion](#)

gen contents do not vary independently, these results are only suggestive of observed relationships. Additional testing with more varied fuel composition are needed to fully address fuel composition effects on soot formation.

3.4 Aged emissions

5 As the distance from the engine increases, the plume temperature decreases and less-volatile emission species begin to condense, either to form new particles or as coatings on existing soot particles. As shown in Fig. 6, only soot-mode particles (80–100 nm) are measured at the exhaust plane while additional nucleation-mode particles (10–40 nm) are observed downwind. These result in large increases in EI_N and EI_V between 1 and 30 m (Fig. 7). Up to a 50% increase in EI_N is seen between 30 and 145 m but no significant increase in EI_V . This suggests that any particles formed between 30 m and 145 m are likely small. Further downwind, these particles are likely to coagulate causing a drop in EI_N while EI_V remains constant.

15 Comparing the emission indices at 30 m from all runs (for JP-8 in Fig. 8), a large spread is seen in the values due to differences in ambient temperature. As ambient temperature increases aerosol number concentration clearly decreases. To examine the ambient temperature impact more closely, a linear fit of EI_N versus temperature was plotted for each power (Supplement). The y-intercept (and its error) gives the emission index at 0°C (and its error), while the slope (and its error) gives the temperature dependence (and its error) in $\#(\text{kgfuel})^{-1}\text{°C}^{-1}$. The EI_N at 15°C can then be calculated (15°C is chosen because it is the ICAO standard temperature). The EI_N (15°C) decreases with power (Fig. 9) as a result of reduced precursor UHC emission (which results in less nucleation). The temperature dependence is always negative representing a decrease in nucleation as the ambient temperature increases. The temperature-dependency is most pronounced at low power but is relatively constant at all other powers.

25 A similar analysis can be performed for the aerosol volume data (Fig. 10). The total aerosol volume decreases from low to mid-power due to a decrease in the formation of

Reductions in aircraft particulate emissions

A. J. Beyersdorf et al.

Title Page

Abstract

Introduction

Conclusions

References

Tables

Figures



Back

Close

Full Screen / Esc

Printer-friendly Version

Interactive Discussion



volatile aerosols. However, the aerosol volume increases at powers greater than 65 % due to increased soot production at these powers. A strong temperature dependence of the total aerosol volume is seen at low power but the dependence is negligible at higher powers. The El_V measurements are a composite of both nucleation-mode particles and soot-mode particles (which in turn are composed of black carbon and any volatile coating). To determine the importance of these components, the nucleation and soot modes are fitted with a bimodal log-normal fit. The volume emissions indices for the two separate modes are shown in Fig. 10. Nucleation-mode volume is similar to the trend for gas-phase UHC emissions with greatest El_V at low power. As the power increases, the engines produce less hydrocarbons and the mass of volatile aerosols decreases. Sulfur dioxide (also a volatile aerosol precursor) is fairly constant with power and thus not responsible for the decrease in volatile mass. Temperature effects for the nucleation-mode volume are most important at low power.

Conversely, the soot-mode particle number concentration increases as power increases. This soot-mode is composed of both the soot and its coating. The trend in soot-mode El_V is similar to the El_{BC} trend (Fig. 3). However, to compare the soot El_V and black carbon El_{BC} quantitatively requires the density of the black carbon to be known. At the exhaust plane, the aerosol is composed entirely of soot and the data in Fig. 5 suggest an average soot density (ρ_{BC}) of 1.1 g cm^{-3} . Black carbon volumes for the 30 m sampling are then found using this density (assuming the density is constant between 1 and 30 m). Calculated emissions of black carbon volumes agree with the total soot-mode aerosol El_V to within $\pm 15 \text{ mm}^3 \text{ kg}^{-1}$ suggesting an upper limit of $15 \text{ mm}^3 \text{ kg}^{-1}$ for the El_V of the soot-mode coating. This would represent just 10% of the total volatile emissions (Fig. 11) at idle conditions but could be significant at high power conditions. The temperature dependence for the soot-mode volume is negligible except at high power. This suggests a higher coating volume than at low power. It is likely that condensation is more pronounced at high power due to the large soot surface area available.

Reductions in aircraft particulate emissions

A. J. Beyersdorf et al.

[Title Page](#)[Abstract](#)[Introduction](#)[Conclusions](#)[References](#)[Tables](#)[Figures](#)[◀](#)[▶](#)[◀](#)[▶](#)[Back](#)[Close](#)[Full Screen / Esc](#)[Printer-friendly Version](#)[Interactive Discussion](#)

The volatile aerosol volume emission index ($El_{\text{Volatile-V}}$) can be determined based on the total El_V , the El_{BC} and the soot density

$$El_{\text{Volatile-V}} = El_V - El_{\text{BC}} \cdot \rho_{\text{BC}} \quad (2)$$

This then gives the volatile aerosol mass emission index ($El_{\text{Volatile-M}}$) using a volatile aerosol density of 1.2 g cm^{-3} based on the literature review of Turpin and Lim (2001). Aerosol mass spectrometer (AMS) measurements showed that volatile aerosol composition was dependent on the gas-phase precursors in the exhaust. Both gas-phase (Fig. 2) and particulate organics (Fig. 11) are highest at low power and decrease rapidly for powers greater than 15%. Conversely, SO_2 and particulate sulfate vary less than 10% with power. Thus at engine idle, organics dominate the volatile PM; while at take-off power, sulfates represent 30% of the volatile mass.

Significant reductions in volatile aerosol formation are expected for the alternative fuels due to dramatically lower precursor gas emissions (SO_2 and hydrocarbons). A significant reduction in El_N was measured for the pure FT fuels of 94%, similar to that measured directly behind the engine (Fig. 12). However, reductions for the blended fuels measured downwind (30–44%) were significantly less reduced than measured at the exhaust plane (64%). This result is not unusual; Timko et al. (2010) observed higher relative El_N in a plume generated by combustion of 50% synthetic fuel. From modelling analysis Timko et al. showed that the reduced availability of soot surface area in the blended fuel exhaust caused new particle formation to be favored over condensation of volatile material on to soot-mode particles. For the pure FT fuels, precursors are low enough that El_N reductions are still large. Alternatively, El_V trends are dominated by the reductions in soot between the fuels with reductions of 79–86% for the FT fuels and 36–46% for the blends.

A shift in volatile aerosol composition was measured when the alternative fuels were used. Particulate sulfate EIs were near zero for the FT fuels as a result of the lower fuel sulfur and subsequent SO_2 emissions (Fig. 2). A reduction in organics was also measured for the alternative fuels consistent with the reductions in gas-phase UHC.

Reductions in aircraft particulate emissions

A. J. Beyersdorf et al.

[Title Page](#)[Abstract](#)[Introduction](#)[Conclusions](#)[References](#)[Tables](#)[Figures](#)[Back](#)[Close](#)[Full Screen / Esc](#)[Printer-friendly Version](#)[Interactive Discussion](#)

3.5 Gas-phase-to-volatile-aerosol conversion efficiency

Volatile aerosol measured downwind can be attributed to gas-to-particle conversion of the gas-phase precursors emitted by the engine. As discussed earlier, volatile aerosol formation was most pronounced at low power when gas-phase precursors are at their maximum (Fig. 13). A gas-phase-to-volatile-aerosol conversion efficiency can be defined as

$$\text{Conversion Efficiency} = \frac{EI_{\text{volatile-M}} \times 100\%}{EI_{\text{UHC}} + EI_{\text{SO}_2}}. \quad (3)$$

EI_{UHC} and EI_{SO_2} are measured at 1 m before any volatile aerosols form. The measured SO_2 does not include fuel sulfur converted into SO_3 in the aircraft engine. However, this is likely a small contribution (0.1–1 %; Timko et al., 2013). The fuel sulfur converted to SO_3 is the first to form particulate sulfate; SO_2 measured in the plume must be oxidized to SO_3 before partitioning into the aerosol phase.

Comparing each of the fuels, the efficiency follows a similar trend with low efficiencies at low and high power (0–1.5 %) and maximum conversion at mid-power (1.5–4 %). The increase from low to mid-power is likely the result of changes in hydrocarbon speciation with power (Beyersdorf et al., 2012). At low power, gaseous hydrocarbons are dominated by alkenes; while with an increase in power, aromatics begin to dominate the hydrocarbon speciation. While alkenes are more likely to be oxidized than aromatics, the oxidation products of aromatics (compared to those from alkenes) are more likely to partition to the aerosol phase because of potentially lower volatilities. The decrease in conversion efficiency above 45 % power is likely a result of the continuing decrease in hydrocarbon emissions. Compared to hydrocarbons, sulfur dioxide emission indices are fairly constant with power. Thus at the highest powers the precursor emissions are dominated by sulfur dioxide. Conversion efficiencies at these high powers are consistent with measurements of the SO_2 -to- SO_3 conversion in engines (0.1–1 %; Timko et al., 2013).

4 Conclusions

The potential use of FT fuels as aviation fuel is driven by the goal of reducing dependence on foreign oil and for the development of sustainable fuel sources. A beneficial impact of alternative jet fuels is a decrease in particulate and gas-phase emissions.

5 Significant reductions on the order of 90 % were seen in aerosol emissions when using the neat Fischer–Tropsch fuels. During the test, no marked differences were seen in engine performance between the fuels. However, fuel leaks occurred in the aircraft fuel system and tanker trucks for the neat FT fuels. This was due to the absence of aromatic compounds, which have been shown to increase seal swell. For this and other
10 reasons (e.g. the neat FT fuels studied do not meet the minimum density specifications for aviation fuels) the initial alternative fuels used for aviation will likely be blends with standard jet fuel.

Volatile aerosol formed rapidly within the first 30 m downwind of the engine. Formation was most significant at low power when precursors are the most abundant.
15 Aerosol volume (and mass) was significantly reduced for all the neat alternative fuels and blends with JP-8, while El_N was only significantly reduced for the neat FT fuels. Volatile aerosol formation was highly dependent on ambient temperature especially at low powers. This can have large effects on local air quality surrounding airports in cold regions. Aircraft produced aerosols in these regions will be much larger than levels
20 expected based solely on measurements made directly at the engine exit plane.

The particulate emission reductions associated with FT fuel usage may have significant impacts to air quality and radiation budgets. Decreased ground-level particulate emissions are beneficial for local air quality. The reduction in soot size and sulfur-based emissions for alternative fuels will reduce the soot's potential to act as cloud condensation nuclei (CCN). This, along with reductions in total soot emissions, should cause
25 a decrease in contrail formation for aircraft utilizing FT fuels. Conversely, the smaller size and reduced CCN activation will cause an increase in the atmospheric lifetime of

Reductions in aircraft particulate emissions

A. J. Beyersdorf et al.

Title Page

Abstract

Introduction

Conclusions

References

Tables

Figures



Back

Close

Full Screen / Esc

Printer-friendly Version

Interactive Discussion



the soot. Both of these roles of smaller soot (lower CCN activity but longer lifetime) must be taken into account in modelling of aircraft emissions radiation budget.

Considering solely the particulate emissions, alternative fuels will result in decreased radiative forcing (soot and contrails have positive radiative forcings that are greater than the negative forcing from sulfate emissions; Lee et al., 2009). However, some benefits from the reductions may be offset by increased CO₂ emissions during FT fuel production. Thus emissions during both the production and use must be further analyzed to determine the true benefits of alternative aviation fuels. The use of bio-feedstocks in addition to CCS technology could reduce the energy of production penalty. Regardless of the feedstock, the reductions in particulate emissions measured here are expected for all alternative fuels with similar fuel composition changes.

Supplementary material related to this article is available online at:
<http://www.atmos-chem-phys-discuss.net/13/15105/2013/acpd-13-15105-2013-supplement.pdf>.

Acknowledgements. We would like to thank the sponsorship of the NASA Fundamental Aeronautics Program and Subsonic Fixed Wing Project, the support of the NASA Dryden Aircraft Operations Facility and the entire AAFEX science team.

References

Anderson, B. E., Beyersdorf, A. J., Hudgins, C. H., Plant, J. V., Thornhill, K. L., Winstead, E. L., Ziemba, L. D., Howard, R., Corporan, E., Miake-Lye, R. C., Herndon, S. C., Timko, M., Woods, E., Dodds, W., Lee, B., Santoni, G., Whitefield, P., Hagen, D., Lobo, P., Knighton, W. B., Bulzan, D., Tacina, K., Wey, C., VanderWal, R., and Bhargava, A.: Alternative Aviation Fuel Experiment (AAFEX), NASA/TM-2011-217059, NASA Center for AeroSpace Information, Hanover, MD, USA, 2011.

Reductions in aircraft particulate emissions

A. J. Beyersdorf et al.

Title Page

Abstract

Introduction

Conclusions

References

Tables

Figures

⏪

⏩

◀

▶

Back

Close

Full Screen / Esc

Printer-friendly Version

Interactive Discussion



**Reductions in
aircraft particulate
emissions**

A. J. Beyersdorf et al.

Title Page

Abstract

Introduction

Conclusions

References

Tables

Figures

◀

▶

◀

▶

Back

Close

Full Screen / Esc

Printer-friendly Version

Interactive Discussion



- Bauer, S. H. and Jeffers, P. M.: Mechanistic investigation of soot precursors, *Energ. Fuels*, 2, 446–453, 1988.
- Beyersdorf, A. J., Thornhill, K. L., Winstead, E. L., Ziemba, L. D., Blake, D. R., Timko, M. T., and Anderson, B. E.: Power-dependent speciation of volatile organic compounds in aircraft exhaust, *Atmos. Environ.*, 61, 275–282, doi:10.1016/j.atmosenv.2012.07.027, 2012.
- Chin, J. S. and Lefebvre, A. H.: Influence of fuel composition on flame radiation in gas-turbine combustors, *J. Propul. Power*, 6, 497–503, doi:10.2514/3.25462, 1990a.
- Chin, J. S. and Lefebvre, A. H.: Influence of fuel composition-properties on soot emissions from gas-turbine combustors, *Combust. Sci. Technol.*, 73, 479–486, doi:10.1080/00102209008951664, 1990b.
- Corporan, E., DeWitt, M. J., Belovich, V., Pawlik, R., Lynch, A. C., Gord, J. R., and Meyer, T. R.: Emissions characteristics of a turbine engine and research combustor burning a Fischer-Tropsch jet fuel, *Energ. Fuels*, 21, 2615–2626, 2007.
- DeCarlo, P. F., Slowik, J. G., Worsnop, D. R., Davidovits, P., and Jimenez, J. L.: Particle morphology and density characterization by combined mobility and aerodynamic diameter measurements. Part 1: Theory, *Aerosol Sci. Tech.*, 38, 1185–1205, doi:10.1080/027868290903907, 2004.
- DeWitt, M. J., Corporan, E., Graham, J., and Minus, D.: Effects of aromatic type and concentration in Fischer-Tropsch fuel on emissions production and material compatibility, *Energ. Fuels*, 22, 2411–2418, 2008.
- Gysel, M., Laborde, M., Olfert, J. S., Subramanian, R., and Gröhn, A. J.: Effective density of Aquadag and fullerene soot black carbon reference materials used for SP2 calibration, *Atmos. Meas. Tech.*, 4, 2851–2858, doi:10.5194/amt-4-2851-2011, 2011.
- Herndon, S. C., Wood, E., Northway, M. J., Mlake-Lye, R., Thornhill, L., Beyersdorf, A., Anderson, B. E., Dowlin, R., Dodds, W., and Knighton, W. B.: Aircraft hydrocarbon emissions at Oakland International Airport, *Environ. Sci. Technol.*, 43, 1730–1736, 2009.
- Jaramillo, P., Griffin, W. M., and Matthews, H. S.: Comparative analysis of the production costs and life-cycle GHG emissions of FT liquid fuels from coal and natural gas, *Environ. Sci. Technol.*, 42, 7561–7565, 2008.
- Kinsey, J. S., Timko, M. T., Herndon, S. C., Wood, E. C., Yu, Z. H., Mlake-Lye, R. C., Lobo, P., Whitefield, P., Hagen, D., Wey, C., Anderson, B. E., Beyersdorf, A. J., Hudgins, C. H., Thornhill, K. L., Winstead, E., Howard, R., Bulzan, D. I., Tacina, K. B., and Knighton, W. B.: Determination of the emissions from an aircraft Auxiliary Power Unit (APU)

Reductions in aircraft particulate emissions

A. J. Beyersdorf et al.

Title Page

Abstract

Introduction

Conclusions

References

Tables

Figures

◀

▶

◀

▶

Back

Close

Full Screen / Esc

Printer-friendly Version

Interactive Discussion



during the Alternative Aviation Fuel Experiment (AAFEX), *J. Air Waste Manage.*, 62, 420–430, doi:10.1080/10473289.2012.655884, 2012.

Law, C. K.: Fuel options for next-generation chemical propulsion, *AIAA J.*, 50, 19–36, doi:10.2514/1.J051328, 2012.

5 Lee, D. S., Fahey, D. W., Forster, P. M., Newton, P. J., Wit, R. C. N., Lim, L. L., Owen, B., and Sausen, R.: Aviation and global climate change in the 21st century, *Atmos. Environ.*, 43, 3520–3537, 2009.

10 Lee, B. H., Santoni, G. W., Wood, E. C., Herndon, S. C., Miake-Lye, R. C., Zahniser, M. S., Wofsy, S. C., and Lee, J. W. M.: Measurements of nitrous acid in commercial aircraft exhaust at the Alternative Aviation Fuel Experiment, *Environ. Sci. Technol.*, 45, 7648–7654, doi:10.1021/es200921t, 2011.

Lobo, P., Hagen, D. E., and Whitefield, P. D.: Comparison of PM emissions from a commercial jet engine burning conventional, biomass, and Fischer–Tropsch fuels, *Environ. Sci. Technol.*, 45, 10744–10749, doi:10.1021/es201902e, 2011.

15 Lukachko, S. P., Waitz, I. A., Miake-Lye, R. C., and Brown, R. C.: Engine design and operational impacts on particulate matter precursor emissions, *J. Eng. Gas Turb. Power*, 130, 021505, doi:10.1115/1.2795758, 2008.

20 McEnally, C. S. and Pfefferle, L. D.: Experimental assessment of naphthalene formation mechanisms in non-premixed flames, *Combust. Sci. Technol.*, 128, 257–278, doi:10.1080/00102209708935712, 1997.

Moteki, N. and Kondo, Y.: Dependence of laser-induced incandescence on physical properties of black carbon aerosols: measurements and theoretical interpretation, *Aerosol Sci. Tech.*, 44, 663–675, doi:10.1080/02786826.2010.484450, 2010.

25 Onasch, T. B., Jayne, J. T., Herndon, S., Worsnop, D. R., Miake-Lye, R. C., Mortimer, I. P., and Anderson, B. E.: Chemical properties of aircraft engine particulate exhaust emissions, *J. Propul. Power*, 25, 1121–1137, 2009.

Ramanathan, V. and Carmichael, G.: Global and regional climate changes due to black carbon, *Nat. Geosci.*, 1, 221–227, doi:10.1038/ngeo156, 2008.

30 Richter, H. and Howard, J. B.: Formation of polycyclic aromatic hydrocarbons and their growth to soot – a review of chemical reaction pathways, *Prog. Energ. Combust.*, 26, 565–608, 2000.

Rosfjord, T. J.: Role of fuel chemical-properties on combustor radiative heat load, *J. Propul. Power*, 3, 494–501, doi:10.2514/3.23016, 1987.

**Reductions in
aircraft particulate
emissions**

A. J. Beyersdorf et al.

Title Page

Abstract

Introduction

Conclusions

References

Tables

Figures

◀

▶

◀

▶

Back

Close

Full Screen / Esc

Printer-friendly Version

Interactive Discussion



Sampath, P., Gratton, M., Kretschmer, D., and Odgers, J.: Fuel property effects upon exhaust smoke and the weak extinction characteristics of the Pratt and Whitney PT6A-65 engine, *J. Eng. Gas Turb. Power*, 108, 175–181, 1986.

Santoni, G. W., Lee, B. H., Wood, E. C., Herndon, S. C., Miake-Lye, R. C., Wofsy, S. C., McManus, J. B., Nelson, D. D., and Zahniser, M. S.: Aircraft emissions of methane and nitrous oxide during the Alternative Aviation Fuel Experiment, *Environ. Sci. Technol.*, 45, 7075–7082, doi:10.1021/es200897h, 2011.

Thaiyasuit, P., Pianthong, K., and Milton, B.: Combustion efficiency and performance of RSO biodiesel as alternative fuel in a single cylinder CI engine, *Energ. Explor. Exploit.*, 30, 153–166, 2012.

Timko, M. T., Yu, Z., Onasch, T. B., Wong, H.-W., Miake-Lye, R. C., Beyersdorf, A. J., Anderson, B. E., Thornhill, K. L., Winstead, E. L., Corporan, E., DeWitt, M. J., Klingshirm, C. D., Wey, C., Tacina, K., Liscinsky, D. S., Howard, R., and Bhargava, A.: Particulate emissions of gas turbine engine combustion of a Fischer–Tropsch synthetic fuel, *Energ. Fuels*, 24, 5883–5896, doi:10.1021/ef100727t, 2010.

Timko, M. T., Fortner, E., Franklin, J., Yu, Z., Wong, H.-W., Onasch, T. B., Miake-Lye, R. C., and Herndon, S. C.: Atmospheric measurements of the physical evolution of aircraft exhaust plumes, *Environ. Sci. Technol.*, 47, 3513–3520, 2013.

Tremmel, H. G. and Schumann, U.: Model simulations of fuel sulfur conversion efficiencies in an aircraft engine: dependence on reaction rate constants and initial species mixing ratios, *Aerosp. Sci. Technol.*, 3, 417–430, doi:10.1016/S1270-9638(99)00101-7, 1999.

Turpin, B. J. and Lim, H.-J.: Species contributions to $PM_{2.5}$ mass concentrations: revisiting common assumptions for estimating organic mass, *Aerosol Sci. Tech.*, 35, 602–610, 2001.

Wang, H. and Frenklach, M.: Calculations of rate coefficients for the chemically activated reactions of acetylene with vinylic and aromatic radicals, *J. Phys. Chem.*, 98, 11465–11489, 1994.

Wey, C. C., Anderson, B. E., Wey, C., Miake-Lye, R. C., Whitefield, P., and Howard, R.: Overview of the Aircraft Particle Emissions Experiment, *J. Propul. Power*, 23, 898–905, 2007.

Xie, X., Wang, M., and Han, J.: Assessment of fuel-cycle energy use and greenhouse gas emissions for Fischer–Tropsch diesel from coal and cellulosic biomass, *Environ. Sci. Technol.*, 45, 3047–3053, doi:10.1021/es1017703, 2011.

Yu, Z. H., Herndon, S. C., Ziemba, L. D., Timko, M. T., Liscinsky, D. S., Anderson, B. E., and Miake-Lye, R. C.: Identification of lubrication oil in the particulate matter emissions from

engine exhaust of in-service commercial aircraft, Environ. Sci. Technol., 46, 9630–9637, 2012.

Discussion Paper | Discussion Paper | Discussion Paper | Discussion Paper | Discussion Paper

ACPD

13, 15105–15139, 2013

Reductions in aircraft particulate emissions

A. J. Beyersdorf et al.

Title Page

Abstract

Introduction

Conclusions

References

Tables

Figures



Back

Close

Full Screen / Esc

Printer-friendly Version

Interactive Discussion



Reductions in aircraft particulate emissions

A. J. Beyersdorf et al.

Title Page

Abstract

Introduction

Conclusions

References

Tables

Figures

◀

▶

◀

▶

Back

Close

Full Screen / Esc

Printer-friendly Version

Interactive Discussion



Table 1. Measurements used for analysis.

| Parameter | Instrument | Sampling location |
|-------------------------------------------|---------------------------------------------|-------------------|
| Total particle number (> 4 nm) | Condensation Particle Counter (CPC) | 1, 30 and 145 m |
| Total particle number (> 6 nm) | Engine Exhaust Particle Spectrometer (EEPS) | 1 and 30 m |
| Aerosol size distribution (9–310 nm) | Differential Mobility Analyzer (DMA) | 1, 30 and 145 m |
| Black carbon mass | Multi-Angle Absorption Photometer (MAAP) | 1 and 30 m |
| Particulate Sulfate and organic mass | Aerosol Mass Spectrometer (AMS) | 1 and 30 m |
| CO and CO ₂ ^a | Non-Dispersive Infrared Spectroscopy (NDIR) | 1 m |
| Unburned Hydrocarbons (UHCs) ^a | Flame Ionization Detector (FID) | 1 m |
| SO ₂ | UV Fluorescence | 1 m |

^a Used to calculate the combustion efficiency.

Reductions in aircraft particulate emissions

A. J. Beyersdorf et al.

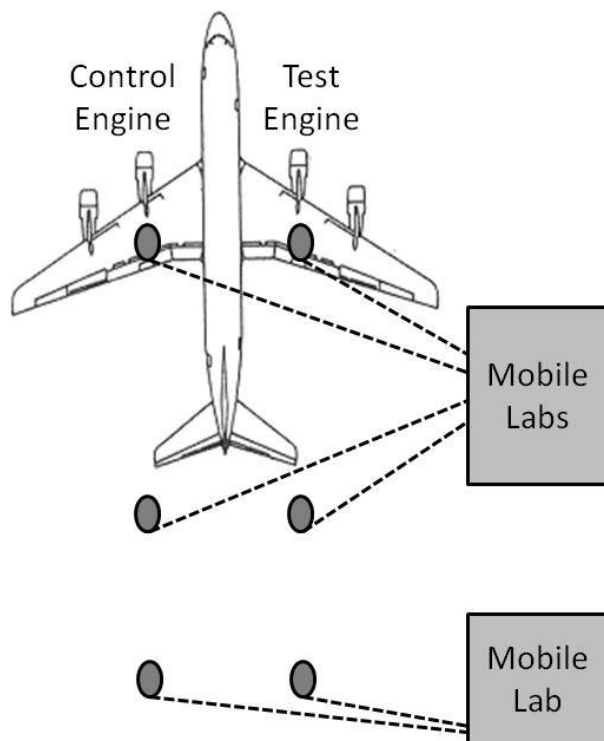


Fig. 1. Diagram of the AAFEX test setup. Exhaust samples were drawn from 1, 30, and 145 m probes (circles; details in Anderson et al., 2011) mounted behind both the control engine (left, inboard), which burned only JP-8 fuel, and the test engine (right, inboard), which burned JP-8 and alternative fuels. Five mobile labs contained instrumentation for the 1 m and 30 m probes, while a separate lab contained instrumentation specifically for the 145 m probe. Probe distances are not drawn to scale.

Title Page

Abstract

Introduction

Conclusions

References

Tables

Figures

◀

▶

◀

▶

Back

Close

Full Screen / Esc

Printer-friendly Version

Interactive Discussion



Reductions in aircraft particulate emissions

A. J. Beyersdorf et al.

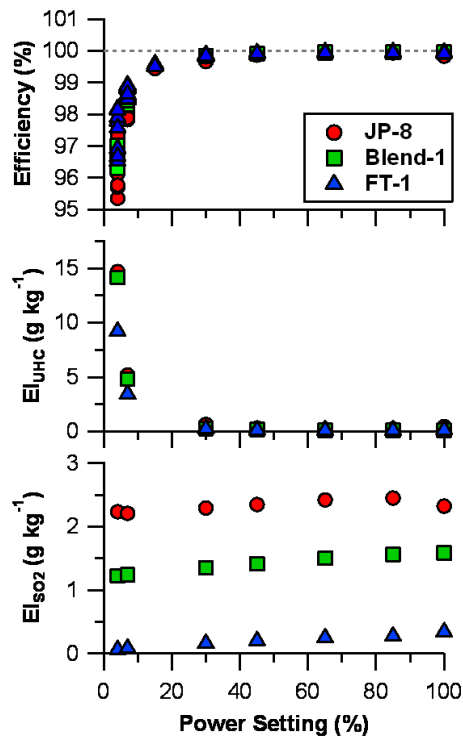


Fig. 2. Combustion efficiency, EI_{UHC} and EI_{SO_2} as a function of engine power for JP-8 and FT-1 fuels. FT-2 and Blend-2 results were similar to FT-1 and Blend-1 measurements. Combustion efficiency was calculated based on the CO and unburned hydrocarbons.

[Title Page](#)
[Abstract](#)
[Introduction](#)
[Conclusions](#)
[References](#)
[Tables](#)
[Figures](#)
[◀](#)
[▶](#)
[◀](#)
[▶](#)
[Back](#)
[Close](#)
[Full Screen / Esc](#)
[Printer-friendly Version](#)
[Interactive Discussion](#)


Reductions in aircraft particulate emissions

A. J. Beyersdorf et al.

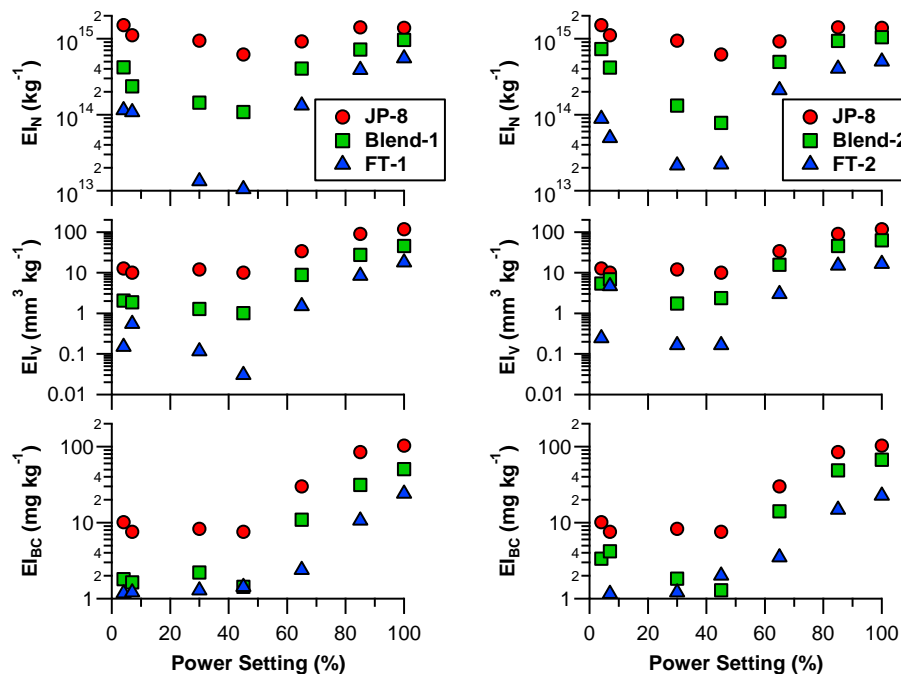


Fig. 3. Aerosol emission indices 1 m behind the #3 engine when fuelled with JP-8, blended fuels and pure FT fuels for FT-1 (left) and FT-2 (right).

Title Page

Abstract

Introduction

Conclusions

References

Tables

Figures

◀

▶

◀

▶

Back

Close

Full Screen / Esc

Printer-friendly Version

Interactive Discussion



Reductions in
aircraft particulate
emissions

A. J. Beyersdorf et al.

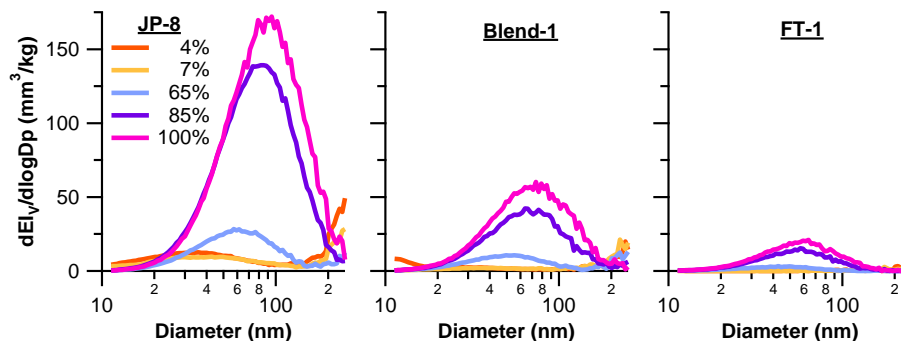


Fig. 4. Volume-weighted size distributions at 1 m behind the exhaust plane for JP-8, Blend-1 and FT-1 (size distributions for Blend-2 and FT-2 are similar).

[Title Page](#)[Abstract](#)[Introduction](#)[Conclusions](#)[References](#)[Tables](#)[Figures](#)[⏪](#)[⏩](#)[◀](#)[▶](#)[Back](#)[Close](#)[Full Screen / Esc](#)[Printer-friendly Version](#)[Interactive Discussion](#)

Reductions in
aircraft particulate
emissions

A. J. Beyersdorf et al.

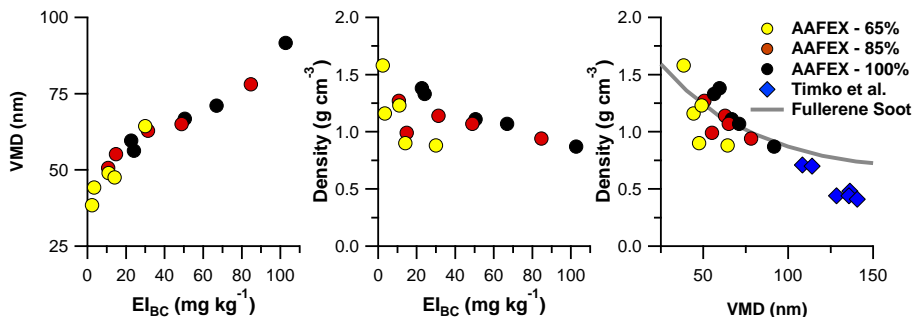


Fig. 5. Soot VMD increases (left) and density decreases (center) as EI_{BC} increases for the AAFEX dataset (1 m behind the engine). Only 65–100% power settings were used because of low loadings below 65%. Fuel type is not differentiated but the pure FT fuels are those with the lowest black carbon loadings at each power. Plotting density versus VMD (right) allows for comparison with aircraft emission measurements by Timko et al. (2010) and laboratory studies of fullerene soot (Gysel et al., 2011).

[Title Page](#)[Abstract](#)[Introduction](#)[Conclusions](#)[References](#)[Tables](#)[Figures](#)[◀](#)[▶](#)[◀](#)[▶](#)[Back](#)[Close](#)[Full Screen / Esc](#)[Printer-friendly Version](#)[Interactive Discussion](#)

Reductions in aircraft particulate emissions

A. J. Beyersdorf et al.

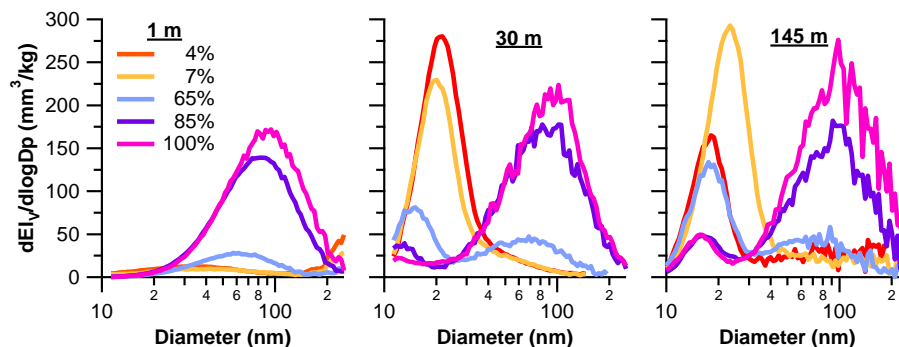


Fig. 6. Volume-weighted size distributions at 1, 30 and 145 m behind the exhaust plane for JP-8 fuel during one engine test (i.e. at constant ambient temperature).

[Title Page](#)[Abstract](#)[Introduction](#)[Conclusions](#)[References](#)[Tables](#)[Figures](#)[⏪](#)[⏩](#)[◀](#)[▶](#)[Back](#)[Close](#)[Full Screen / Esc](#)[Printer-friendly Version](#)[Interactive Discussion](#)

Reductions in aircraft particulate emissions

A. J. Beyersdorf et al.

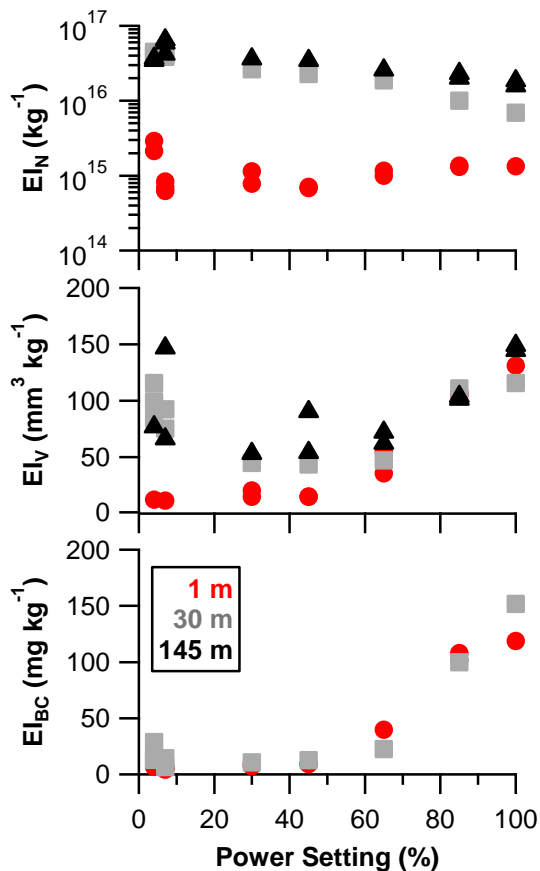


Fig. 7. Number and volume EIs at 1, 30 and 145 m behind the exhaust plane for one engine test (i.e. at constant ambient temperature). Black carbon mass was not measured at the 145 m probe.

Title Page

Abstract

Introduction

Conclusions

References

Tables

Figures

◀

▶

◀

▶

Back

Close

Full Screen / Esc

Printer-friendly Version

Interactive Discussion



Reductions in
aircraft particulate
emissions

A. J. Beyersdorf et al.

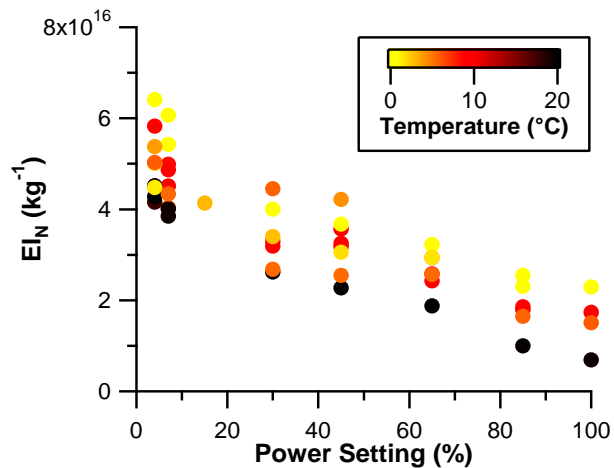


Fig. 8. JP-8 EI_N measured at 30 m from the exhaust plane sorted by the ambient temperature.

[Title Page](#)[Abstract](#)[Introduction](#)[Conclusions](#)[References](#)[Tables](#)[Figures](#)[◀](#)[▶](#)[◀](#)[▶](#)[Back](#)[Close](#)[Full Screen / Esc](#)[Printer-friendly Version](#)[Interactive Discussion](#)

Reductions in aircraft particulate emissions

A. J. Beyersdorf et al.

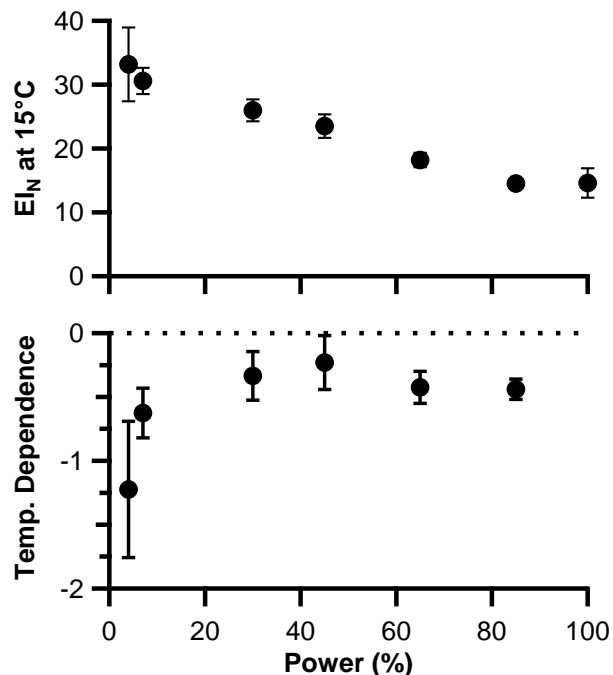


Fig. 9. Aerosol number emission index at 15 °C ($10^{16} \text{ # kg}^{-1}$) and its temperature dependence ($10^{16} \text{ # kg}^{-1} \text{ °C}^{-1}$) as a function of power as measured at the 30 m probe. Error bars are the 1 sigma standard deviation of the linear fits. The temperature dependence for 100 % power is not shown because there is relatively little data.

[Title Page](#)[Abstract](#)[Introduction](#)[Conclusions](#)[References](#)[Tables](#)[Figures](#)[◀](#)[▶](#)[◀](#)[▶](#)[Back](#)[Close](#)[Full Screen / Esc](#)[Printer-friendly Version](#)[Interactive Discussion](#)

Reductions in aircraft particulate emissions

A. J. Beyersdorf et al.

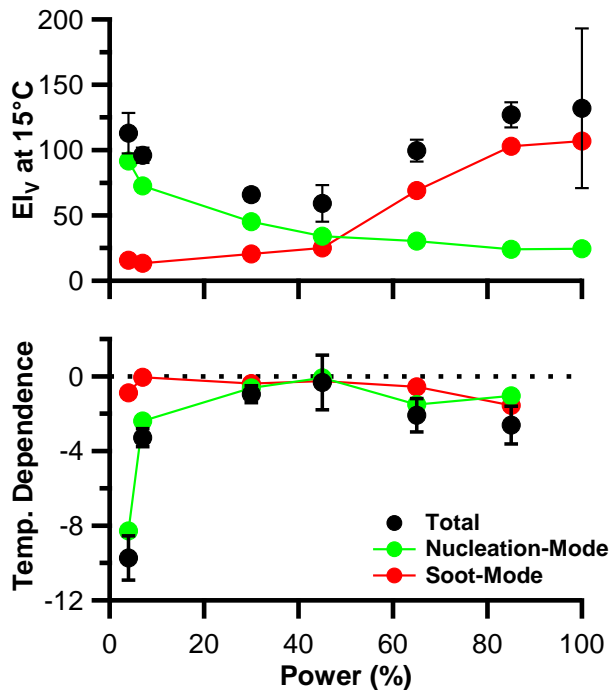


Fig. 10. Total aerosol volume emission index at 15 °C ($\text{mm}^3 \text{kg}^{-1}$) and its temperature dependence ($\text{mm}^3 \text{kg}^{-1} \text{°C}^{-1}$) as a function of power as measured at the 30 m probe. Error bars are the 1 sigma standard deviation of the linear fits for the total aerosol volume.

Reductions in aircraft particulate emissions

A. J. Beyersdorf et al.

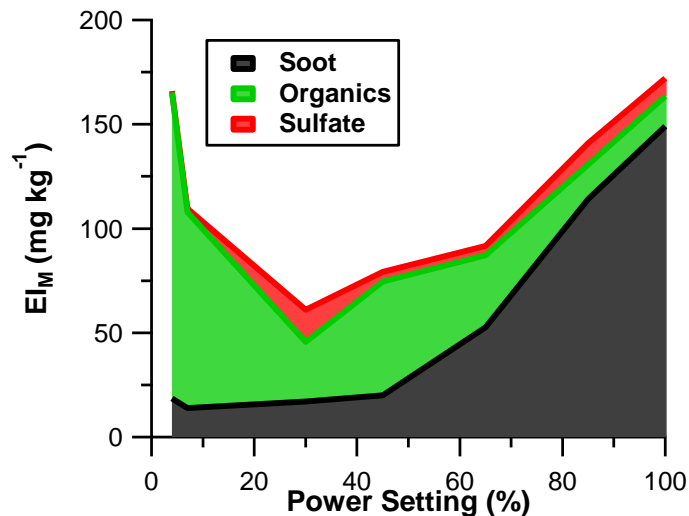


Fig. 11. Chemically-resolved total aerosol mass emission index as a function of engine power. The total EI_M was determined from the EI_V assuming a density of 1.2 g cm^{-3} and the EI_{BC} assuming a density of 1.1 g cm^{-3} . EI_{volatile} is defined as the difference between EI_M and EI_{BC} . EI_{Org} and EI_{SO_4} were then calculated from the AMS organic and sulfate fractions of EI_{volatile} .

[Title Page](#)[Abstract](#)[Introduction](#)[Conclusions](#)[References](#)[Tables](#)[Figures](#)[◀](#)[▶](#)[◀](#)[▶](#)[Back](#)[Close](#)[Full Screen / Esc](#)[Printer-friendly Version](#)[Interactive Discussion](#)

Reductions in aircraft particulate emissions

A. J. Beyersdorf et al.

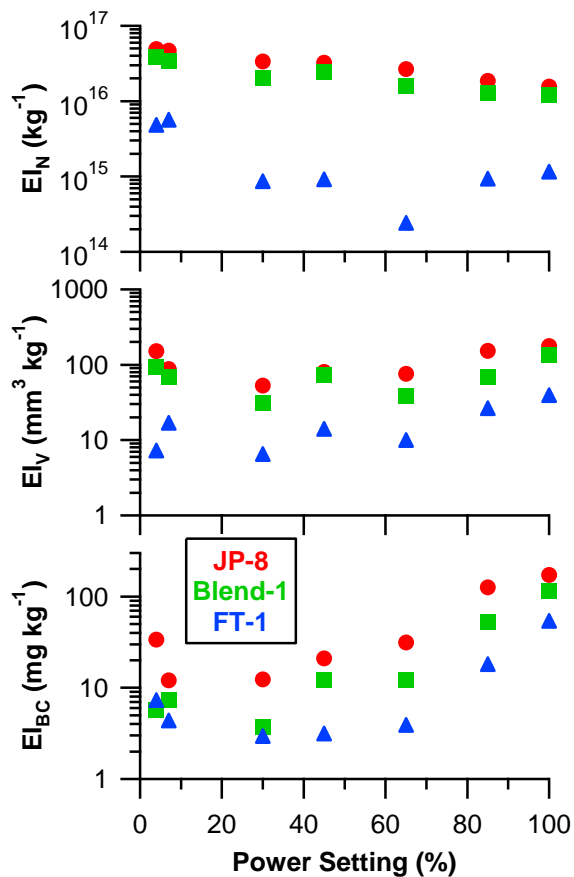


Fig. 12. Emission indices for JP-8, Blend-1 and FT-1 fuel at 30 m behind the engine plane.

Reductions in aircraft particulate emissions

A. J. Beyersdorf et al.

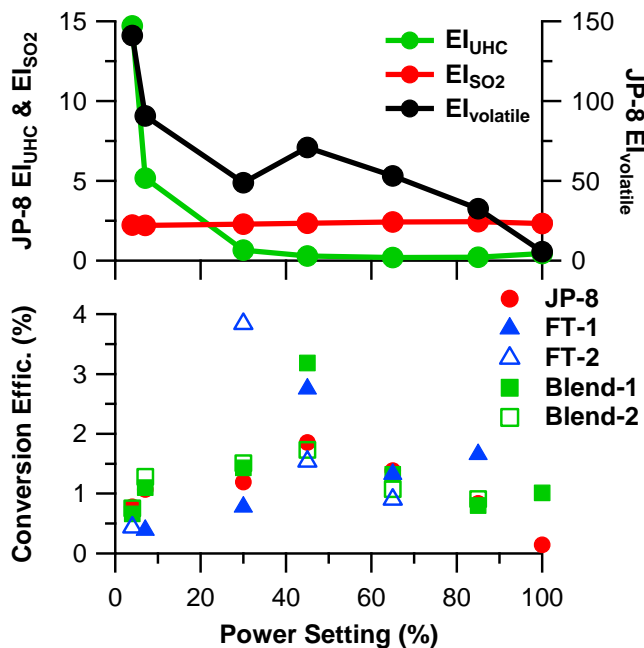


Fig. 13. Emissions indices for gas-phase hydrocarbons (gkg^{-1}), sulfate (gkg^{-1}), and volatile aerosol mass (mgkg^{-1}) for JP-8 (top) and conversion efficiency measured for all the fuels (bottom). Efficiencies for the FT fuels at high power are not included because there was no significant volatile aerosol formation.

Title Page

Abstract Introduction

Conclusions References

Tables Figures

◀ ▶

◀ ▶

Back Close

Full Screen / Esc

Printer-friendly Version

Interactive Discussion

